Paper prepared for the US -Japan Seminar,
Maui, US, November 2-4, 2003

Lateral Resistance, Ductility and Earthquake Response of R/C Frame Strengthened by Multi-Story Steel Brace

KITAYAMA Kazuhiro

ABSTRACT

This paper describes fundamental kinematic characteristics and earthquake response of R/C buildings strengthened by multi-story steel braces. Tests of plane R/C strengthened frames with two-story and three-bay were carried out under cyclic load reversals focusing on the base uplift rotation of the brace and the entire flexural failure at the bottom of the brace caused by tensile yielding of all longitudinal bars in a R/C edge column beside the brace. Moreover, nonlinear static and earthquake response analyses were done for a R/C space building strengthened by a multi-story steel brace to study the effect of bi-lateral earthquake loading on the earthquake resistant performance of the building. Failure mechanism, lateral resistance, deformation capacity and energy dissipation of R/C frames strengthened by a multi-story steel brace were discussed through static tests. It was concluded that earthquake resistant performance of strengthened R/C frames which is controlled by the entire flexural failure at the bottom of a multi-story steel brace was superior to that failed in the brace uplift rotation within the range of drift angle of 2 %. For earthquake response analyses using Kobe earthquake motion records, it was found that drift response against bi-lateral earthquake motions is amplified probably comparing with the response under uni-lateral earthquake loading.

1. INTRODUCTION

For seismic retrofit of existing reinforced concrete (R/C) buildings, steel braces enclosed by perimeter steel rims are often installed into moment resisting open frames. It is most desirable that the one of diagonal chords of steel braces yields in tension and the other buckles in compression under earthquake excitations. Unfortunately the base of a multi-story steel brace may be uplifted and rotate in some cases prior to the yielding or buckling of steel chords depending primarily on the aspect ratio of the span length to the height. In other cases, the strength of a multi-story steel brace is attributed to entire flexural resistance in I-shaped section at the bottom of a unit bay consisting of a steel brace and R/C edge columns, which is induced by tensle yielding of all longitudinal bars in a R/C edge column (called as the failure of Type 3) before the full capacity of a steel brace can be developed.

In the paper, earthquake resistant performance of R/C frames strengthened by a multi-story steel brace, which were designed to develop uplift rotation of a base foundation beneath a multi-story steel brace or the failure of Type 3, was studied by static load reversal tests.

Associate Professor, Graduate School of Engineering, Tokyo Metropolitan University, Dr. Eng.
Email : kitak@ecomp.metro-u.ac.jp

Nonlinear static and earthquake response analyses were, moreover, carried out for a R/C space building strengthened by a multi-story steel brace to study the effect of bi-directional horizontal loads on the earthquake resistant performance of the building.

2. OUTLINE OF TEST

2.1 Specimens

Reinforcement details and section dimensions are shown in **Fig. 1**. Two plane frame specimens with a quarter scale to actual buildings were tested which had three bays with each 1000 mm span length and two stories with the height of 800 mm, placing a multi-story steel brace at the central bay. Section dimensions of R/C beams and columns and steel brace were common for two spcimens except for the amount of longitudinal reinforcement of R/C edge columns beside a steel brace (denoted as Column 2 and 3 in **Fig. 1**).

The failure type of R/C central bay containing a multi-story steel brace was chosen as a test parameter. Specimen No.1 was designed to develop the rotation of base foundation due to the uplift of a multi-story steel brace. On the other hand, Specimen No.2 was designed to result in entire flexural failure at the bottom of a multi-story steel brace which is caused by both yielding of all longitudinal bars in a R/C tensile edge column and pull-out of anchorage bars connecting between horizontal steel rim of a brace and R/C foundation beam. The amount of longitudinal bars in edge columns beside the brace was reduced in Specimen No.2 comparing with those in Specimen No.1 in order to cause the failure of Type 3. Boundary beams and isolated columns were designed according to the weak-beam strong-column concept.

Cross section of a steel brace was a H-shape with 60 mm width and 60 mm depth, which was built by welding flat plates with 6 mm thickness. Details of connection between R/C member and steel rim are illustrated by **Fig. 2**. Anchorage bars of D10 were welded in a row to perimeter steel rims with the center-to-center spacing of 60 mm. Although non-shrinkage mortar is injected between steel rims and R/C members to unify each other for actual practice, mortar injection was omitted in construction of specimens by casting concrete in the state that steel braces were placed at proper position with reinforcement cages of beams and columns. Concrete was cast in the horizontal position using metal casting form. Material properties of steel and concrete are listed in **Table 1**.

2.2 Loading Method And Instrumentation

Table 1 Material properties of steel and concrete

(a) Steel

	Bar size	Yield strength MPa	Young's modulus GPa	Yield strain %
Longitudinal bar in edge column	*D13	336.1	180	0.187
	**D10	367.8	185	0.199
Longitudinal bar in bare column	D13	429.1	179	0.239
Beam longitudinal bar	D13	345.6	184	0.188
Anchorage bar	D10	383.2	188	0.204
Shear reinforcing bar	R6	588.7	207	0.284
Steel brace	flat bar	435.3	208	0.209

* : Specimen No.1 , ** : Specimen No.2

(b)Concrete

Specimen	Compressive strength MPa	Strain at compressive strength %	Secant modulus GPa	Tensile strength MPa
No.1	28.9	0.195	30.5	1.97
No.2	30.3	0.216	28.0	2.43

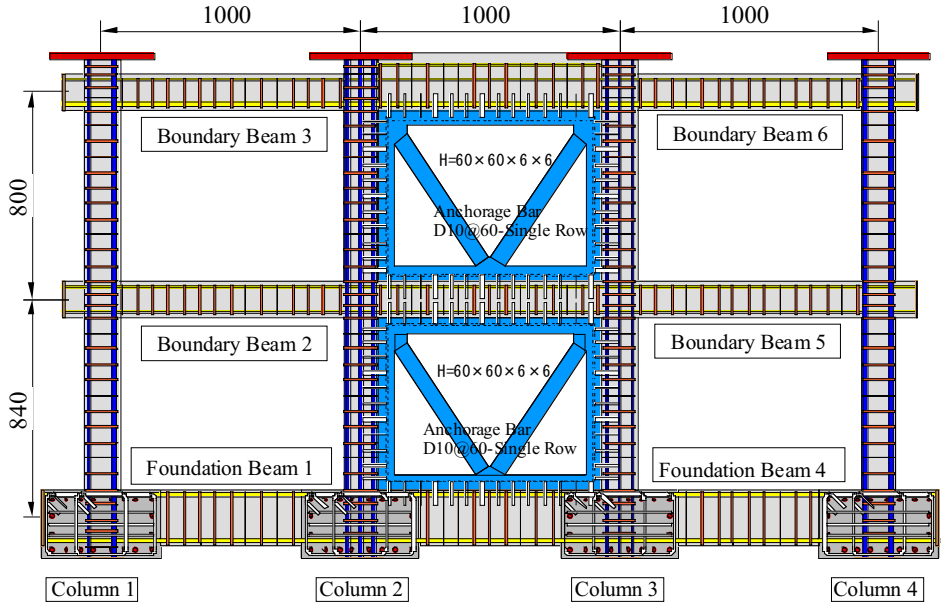

	Boundary Beam(2,3,5,6)	Foundation Beam(1,4)
Section	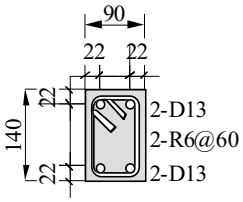	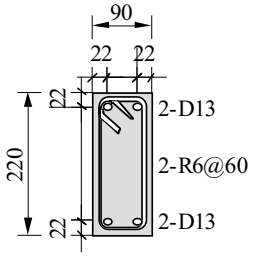
	Pt=2.38% / pw=1.05%	Pt=1.42% / pw=1.05%

	Column 1 and 4 (common)	Column 2 and 3 (Specimen No.1)	Column 2 and 3 (Specimen No.2)
Section	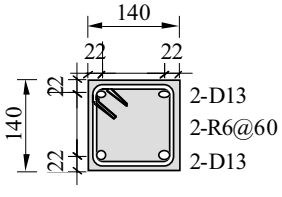	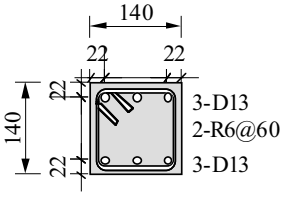	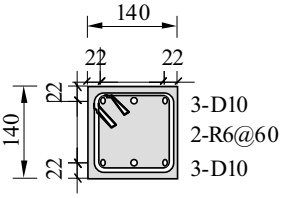
	Pt=1.29% / pw=0.67%	Pt=1.29% / pw=0.67%	Pt=0.73% / pw=0.67%

Fig. 1 Reinforcement details and section dimensions

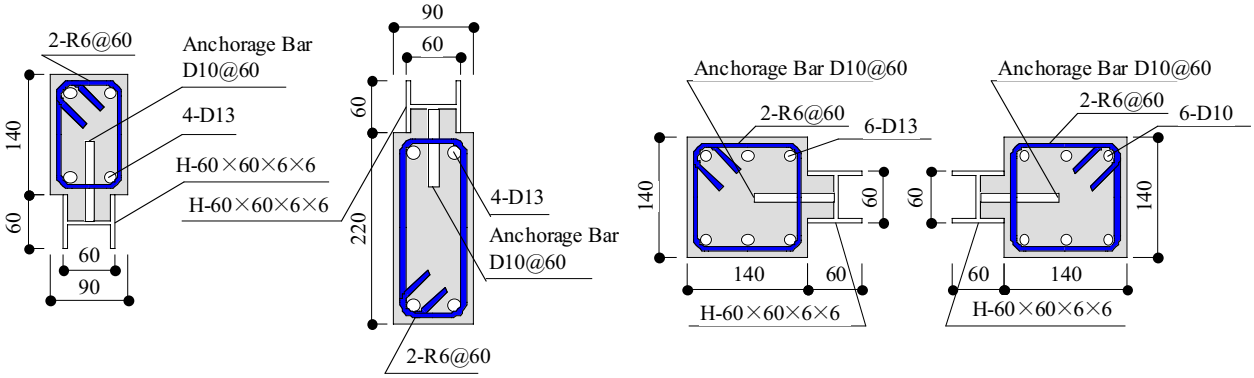

(a) Beam (b) Foundation Beam (c) Column of Specimen No.1 (d) Column of Specimen No.2

Fig. 2 Details of connection between R/C members and steel rim

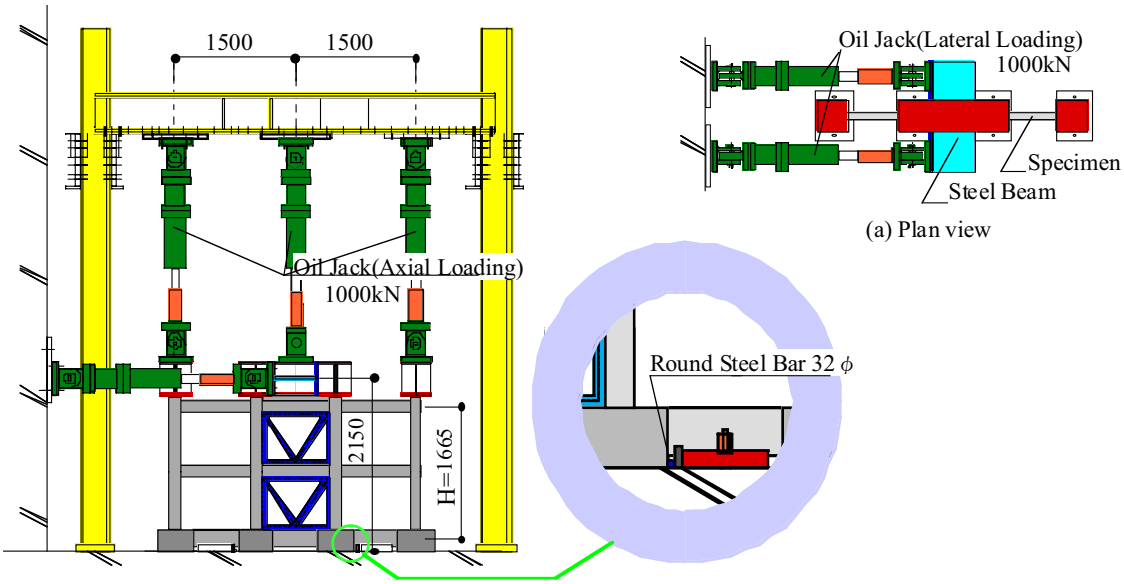

(a) Plan view

(b) Elevation view (c) Close up

Fig. 3 Loading apparatus

The loading system is shown in **Fig. 3**. Top lateral force was applied alone at the center of the specimen by two oil jacks. Each column axial load was kept constant, i.e., 40 kN to isolated columns and 80 kN to edge columns beside a steel brace respectively. Four footings of Specimen No.2 were fixed to R/C reaction floor by PC tendons. For Specimen No.1 designed to cause the uplift of a multi-story steel brace, on the other hand, two footings under the steel brace were not connected to the floor, but lateral reaction force was supported through round steel bar inserted between R/C footing subjected to axial compression and steel reaction plate settled on reaction floor. This testing method was accepted by referring to the study by Kato[1].

Specimen was controlled by the drift angle for one cycle of 0.25 %, two cycles of 0.5 %, 1 % and 2 % respectively and one cycle of 4 %. The drift angle is defined as the horizontal displacement at the center of a top floor beam divided by the height between the center of a foundation beam and a top floor beam, i.e., 1665 mm.

Lateral force and column axial load were measured by load-cells. Horizontal displacement at load applying point and at the center of top and second floor beams, local rotation in a plastic hinge region of beams and columns, and vertical displacement of footings due to uplift of a steel brace were measured by displacement transducers. Strains of beam and column longitudinal bars, vertical and diagonal steel chords of a brace and anchorage bars at the bottom of a first-story steel brace were measured by strain gauges.

3. TEST RESULTS AND DISCUSSIONS

3.1 Process To Failure And Story Shear - Drift Relations

Crack patterns at the end of test are shown in **Fig. 4** and **Photo. 1**. Story shear force - drift angle relations are shown in **Fig. 5** for cyclic load reversals and **Fig. 6** as an envelope curve in positive loading illustrating successive phenomena occurred in the specimen. Story shear force in this paper is defined as the horizontal force applied by oil jacks corrected for the P-Delta effect resulted from column axial load.

3.1.1 Specimen No.1

Uplift of the base foundation under a multi-story steel brace occurred at the drift angle of 0.2 %. Collapse mechanism was formed at the drift angle of 1.4 %, developing flexural yielding at the end of boundary beams and the bottom of first story bare columns. Lateral resistance capacity decayed gradually due to concrete compressive failure at these hinge regions after attaining the peak strength of 215.0 kN at the drift angle of 1 %. Obvious stiffness degradation caused by both base uplift and concrete crushing at hinge regions was observed after sixth loading cycle at the drift angle of 2 % as shown in **Fig. 5 (a)**. Hysteresis loops showed a little pinching shape comparing with those for Specimen No.2.

3.1.2 Specimen No.2

All longitudinal bars in R/C edge column beside a steel brace yielded in tension at the drift angle of 0.3 %. Lateral force resistance reached the maximum capacity of 269.8 kN at the drift angle of 1 %, forming plastic hinges at all boundary beam ends and cracking horizontally at the gap between horizontal steel rim and R/C foundation beam due to pull-out of anchorage bars. Hereafter lateral resistance diminished abruptly by the concrete crushing and the fracture of column longitudinal bars at the bottom of both edge columns at the drift angle of 2 % in eighth loading cycle. Hysteresis loops showed a stable spindle shape until the drift angle of 2 %.

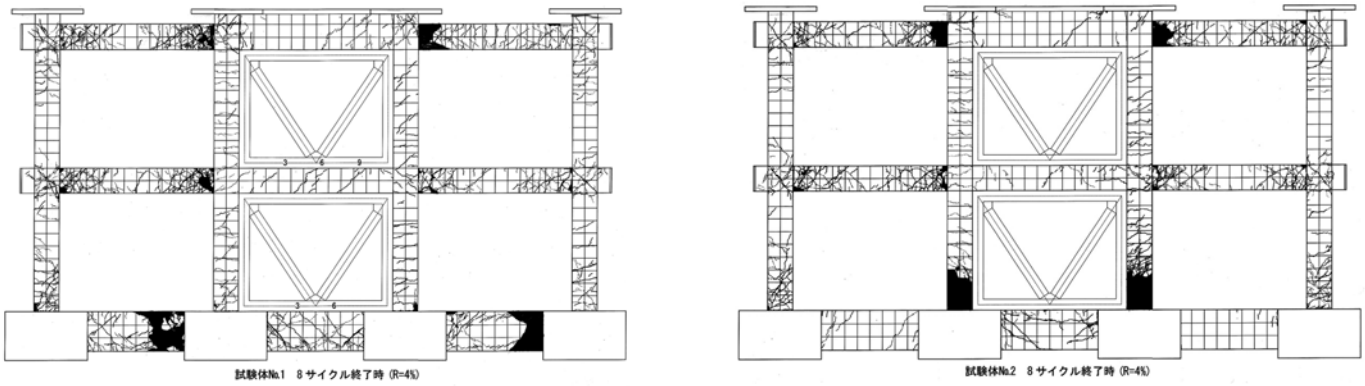

(a) Specimen No.1　　(b) Specimen No.2

Fig. 4 Crack patterns at end of test　　75%

(a) Specimen No.1　　(b) Specimen No.2

Photo. 1 Failure of specimens　　90%

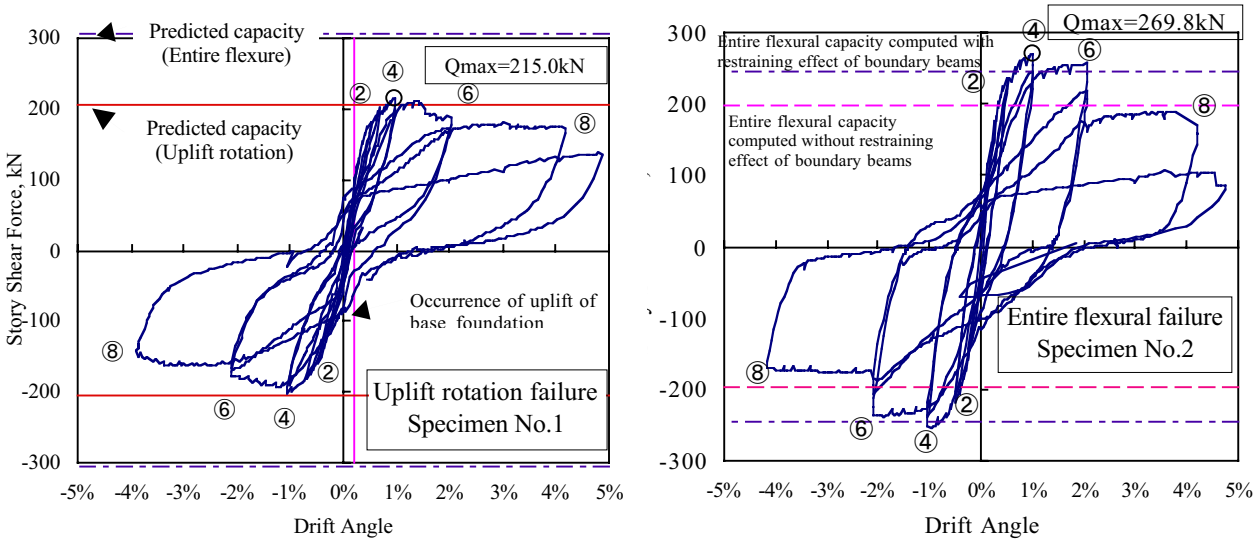

(a) Specimen No.1　　(b) Specimen No.2

Fig. 5 Story shear force- drift angle relations　　81%

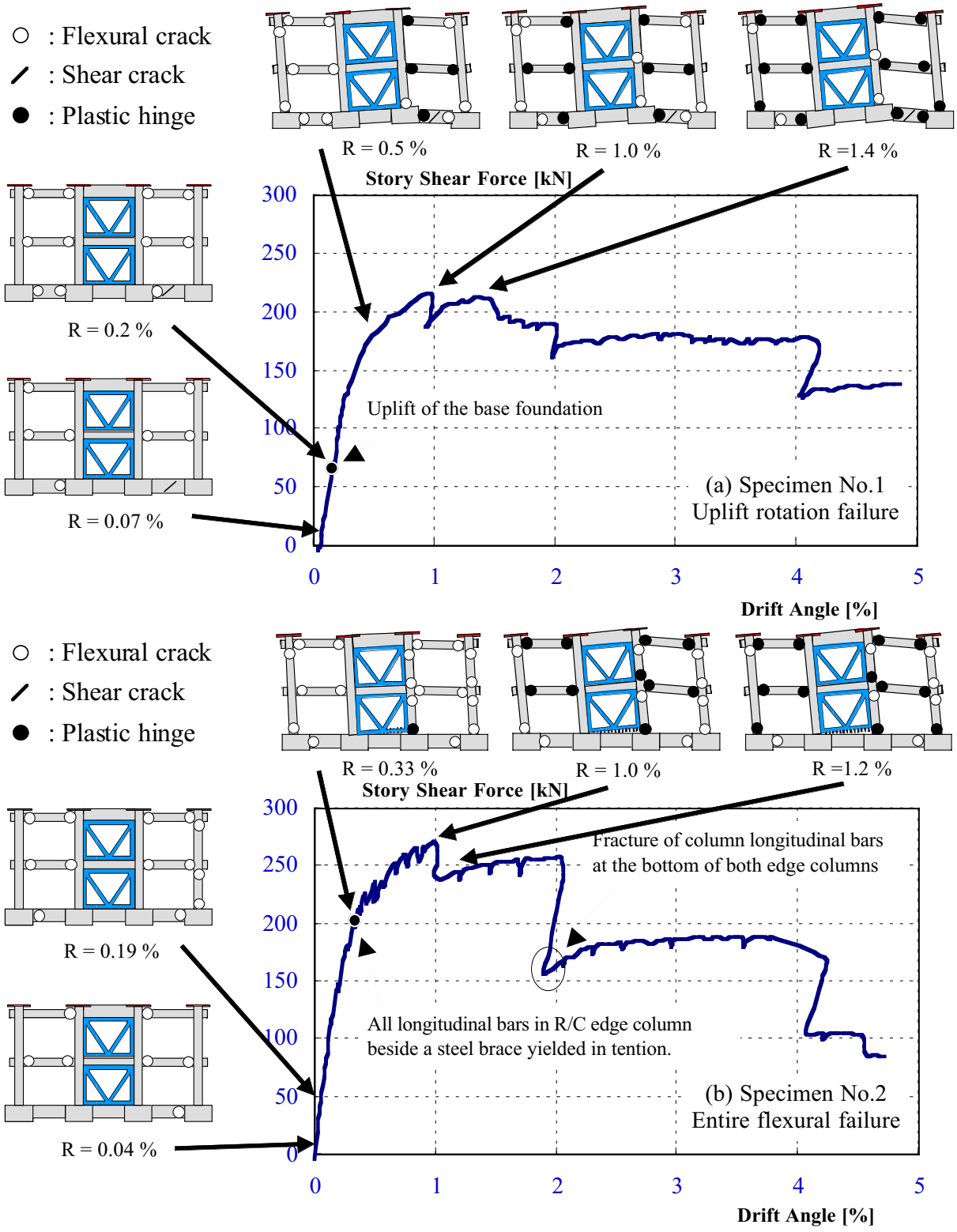

Fig. 6 Envelope curves of story shear force - drift angle relation

3.2 Axial Force Acting On Vertical Steel Rim And R/C Edge Column

Axial force acting on vertical steel rim of the brace, which was computed from measured strain

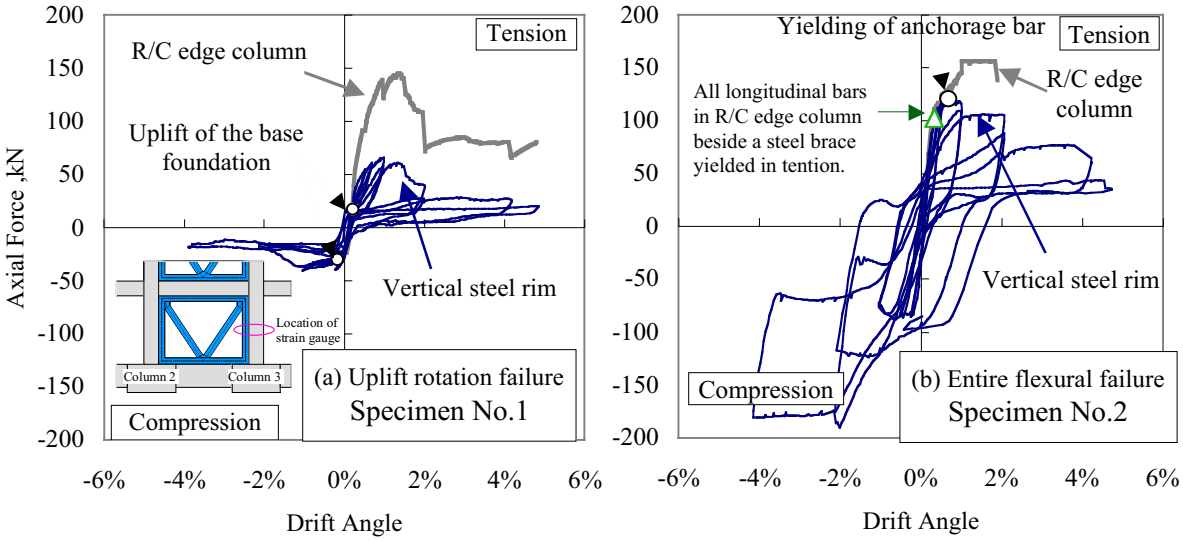

Fig. 7 Axial force acting on vertical steel rim and R/C edge column

80%

at the mid-height in a first story brace, is shown in **Fig. 7**. Vertical steel rims did not yield for both specimens. Tensile axial force induced in R/C edge column beside a brace which was computed by measured strain of longitudinal bars at the mid-height of a first-story edge column is also shown in **Fig. 7**. In Specimen No.2, failed in entire flexure at the bottom of a multi-story steel brace, tensile axial force of vertical steel rim increased even after all longitudinal bars yielded at the bottom of R/C edge column, and attained the peak force with the yielding of anchorage bars at the bottom of the brace. The peak tensile force of vertical steel rim was three-quarters times that of axial force in R/C edge column at the drift angle of 1 %. Therefore it is important to take account of the contribution of vertical steel rim to entire flexural resistance at the bottom of a multi-story steel brace in addition to the longitudinal column bars.

3.3 Lateral Strength

Lateral strength Q_{max} obtained by the test is compared with the computed strength Q_{cal} by Eq.(1) and listed in **Table 2**.

$$Q_{cal} = Q_{c1} + Q_{c4} + Q_{Bf} \qquad (1)$$

where Q_{c1} and Q_{c4} : lateral strength of a R/C isolated column (i.e., Column 1 and Column 4 in **Fig. 8**) computed by Eq.(2) since shear strength was greater than flexural strength for both columns.

$$Q_{c1}, Q_{c4} = \frac{2M_{cu}}{h} \qquad (2)$$

where h : clear height of the column and M_{cu} : ultimate bending moment at column critical

Table 2 Measured and computed lateral strength of specimens

Specimen	Measured Strength (kN)	Computed Strength (kN)				Ratio of computed to measured strength
		Yielding of diagonal chord in brace	Type 3[*] failure	Type 3[**] failure	Brace base rotation failure	
No.1	215.0	490.1	256.9	305.1	205.1	0.95
No.2	269.8	468.3	198.0	246.2	—	[*] 0.73 [**] 0.91

[*] , [**] : Computed lateral strength of Type 3 failure without or with consideration of restraining effect by boundary beams respectively

section which can be computed by Eq.(3).

$$M_{cu} = 0.8a_t \cdot \sigma_y \cdot D + 0.5N_{col} \cdot D\left(1 - \frac{N_{col}}{bD \cdot \sigma_B}\right) \qquad (3)$$

where a_t , σ_y : sectional area and yield strength of tensile longitudinal reinforcement in the column, D : column depth, N_{col} : column axial load, b : column width and σ_B : concrete compressive strength.

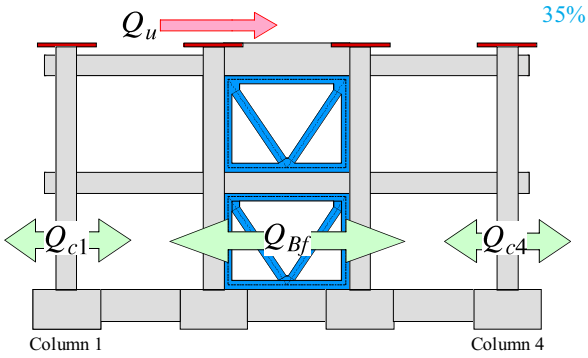

Fig. 8 Lateral resisntance of frame

Q_{Bf} : lateral shear resistance shared by the R/C central bay containing a multi-story steel brace which can be computed by Eq.(4) as illustrated in **Fig. 9**.

For uplift rotation failure,
$$Q_{Bf} = \frac{0.5N_{br} \cdot l_w + \sum_i M_{Bi}}{H} \qquad (4.a)$$

For entire flexural failure (i.e., Type 3),
$$Q_{Bf} = \frac{a_t \cdot \sigma_y \cdot l_w + 0.5N_{br} \cdot l_w + \sum_i M_{Bi}}{H} \qquad (4.b)$$

where a_t , σ_y : sectional area and yield strength of tensile longitudinal reinforcement of edge column beside a steel brace, N_{br} : compressive axial load imposed at the center of a steel brace, l_w : center-to-center distance between R/C edge columns beside a steel brace, $\sum_i M_{Bi}$: sum of the flexural yielding moment of boundary beams framing into a multi-story steel brace, including the restraining moment due to shear force of boundary beams framing into uplift edge column, and H : height between the center of a foundation beam and a top floor beam (1665 mm). It is assumed for Eq.(4) that concentrated roof-level load was applied to the R/C central bay containing a multi-story steel brace.

Lateral strength measured in Specimen No.1 agreed well with that computed by taking account of restraining effect of both boundary and foundation beams on uplift rotation.

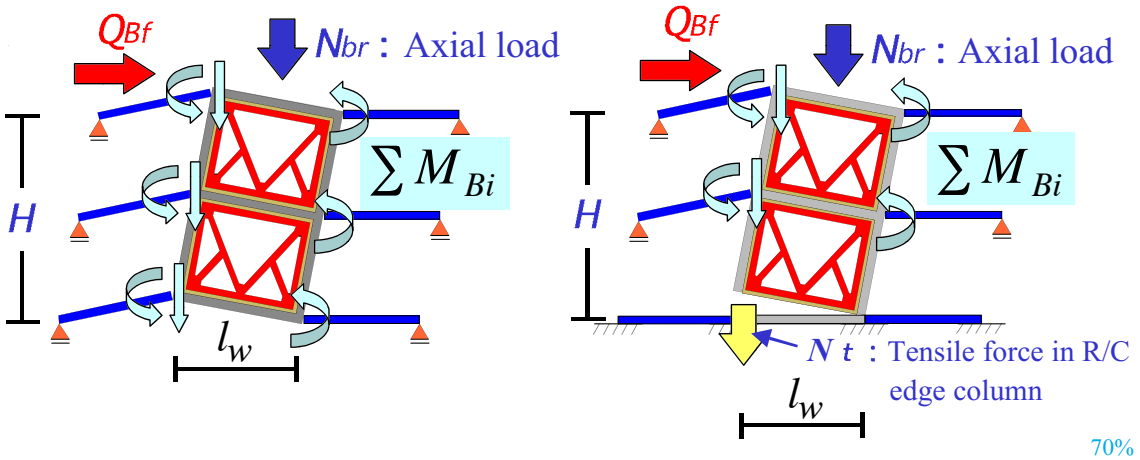

(a) Uplift rotation failure (b) Entire flexural failure

Fig. 9 Lateral shear resistance of R/C unit frame with multi-story steel brace

For Specimen No.2, predicted lateral strength of 198.0 kN without consideration of restraining effect by boundary beams, i.e., lateral shear strength obtained by extracting the term of $\sum_i M_{Bi}$ from Eq.(4.b), was almost equal to measured resistance when all longitudinal bars yielded in a tensile edge column. In the test lateral resistance increased and attained the peak strength with the formation of beam hinge mechanism. Therefore lateral strength for entire flexural failure at the bottom of a multi-story brace was computed by Eq.(4.b) and it was 91 percent of measured lateral strength. It seems that contribution of the vertical steel rim to entire flexural resistance at the bottom of a brace may be considered to the extent that anchorage of a steel brace to R/C foundation beam is effective to carry tensile axial force in vertical steel rim to the foundation.

3.4 Deformation Performance

Standard for evaluation of seismic capacity of existing R/C buildings [2] was revised in 2001 in Japan. Deformation ability for a multi-story steel brace which fails by uplift rotation of the base or entire flexural yielding at the bottom of a brace (i.e., Type 3 failure) can be estimated according to this standard. Deformation ability is expressed by the ductility index denoted as F which is a function of the ductility factor as follows ;

$$F = \frac{\sqrt{2R_{mu}/R_y - 1}}{0.75\left(1 + 0.05R_{mu}/R_y\right)} \qquad (5)$$

where R_{mu} : ultimate story drift angle of R/C members and R_y : yielding story drift angle assumed to be 0.67 %.

The F index for a multi-story steel brace with boundary beams is computed by Eq.(6).

$$F = {}_wq \cdot {}_wF + \Sigma\left({}_bq \cdot {}_bF\right) \qquad (6)$$

where, ${}_wF$, ${}_bF$: ductility index for an isolated steel brace and a boundary beam respectively which can be estimated by Eqs.(7) and (8) and ${}_wq$, ${}_bq$: weighting factor by Eq.(9) to take account of contribution of an isolated brace or boundary beams to total lateral resistance.

for uplift rotation failure, ${}_wF = 3.0$ (7.a)

for entire flexural failure (Type 3), ${}_wF = 2.0$ (7.b)

if ${}_bQ_{su} / {}_bQ_{mu} \le 0.9$, ${}_bF = 1.27$ (8.a)

if ${}_bQ_{su} / {}_bQ_{mu} \ge 1.3$, ${}_bF = 3.5$ (8.b)

if $0.9 \le {}_bQ_{su} / {}_bQ_{mu} \le 1.3$, the ${}_bF$ index shall be computed by the linear interpolation between Eq. (8.a) and Eq.(8.b), where ${}_bQ_{su}$, ${}_bQ_{mu}$: ultimate shear and flexural strength of a boundary beam respectively.

$${}_wq = \frac{{}_wM}{{}_wM + \Sigma {}_bM} \qquad (9.a)$$

$${}_bq = \frac{{}_bM}{{}_wM + \Sigma {}_bM} \qquad (9.b)$$

where ${}_wM$: brace contribution to ultimate resisting moment at the height where the lateral strength of a multi-story steel brace was decided and ${}_bM$: ultimate resisting moment of a boundary beam framing into a multi-story steel brace.

Table 3 Ductility index and ultimate limit drift angle

	R : Limit Drift Angle	Specimen No.1		Specimen No.2	
		Positive Loading	Negative Loading	Positive Loading	Negative Loading
Test Result	R	4.18%	3.36%	3.07%	3.09%
	R(average)	3.77%		3.08%	
Computed Result	F index	2.96		2.38	
	R	2.70%		1.68%	

The F index taken as explained above was 2.96 for Specimen No.1 and 2.38 for Specimen No.2 as listed in **Table 3**. These values correspond to the drift angle of 2.70 % and 1.68 % respectively, which were converted through Eq.(5).

On the other hand, ultimate limit drift angle was obtained in the test as shown in **Fig. 10** which is defined as the drift angle when the lateral resistance descended to 80 % of peak strength for the envelope curve of the story shear force - drift angle relation. Average ultimate limit drift angle for positive and negative loading directions was 3.8 % for Specimen No.1 and 3.1 % for Specimen No.2. This indicates that ductility performance in the case of uplift rotation failure of a multi-story steel brace was superior to that for entire flexural failure due to tensile yielding of all longitudinal bars in a R/C edge column as predicted by the F indices. Computed ultimate

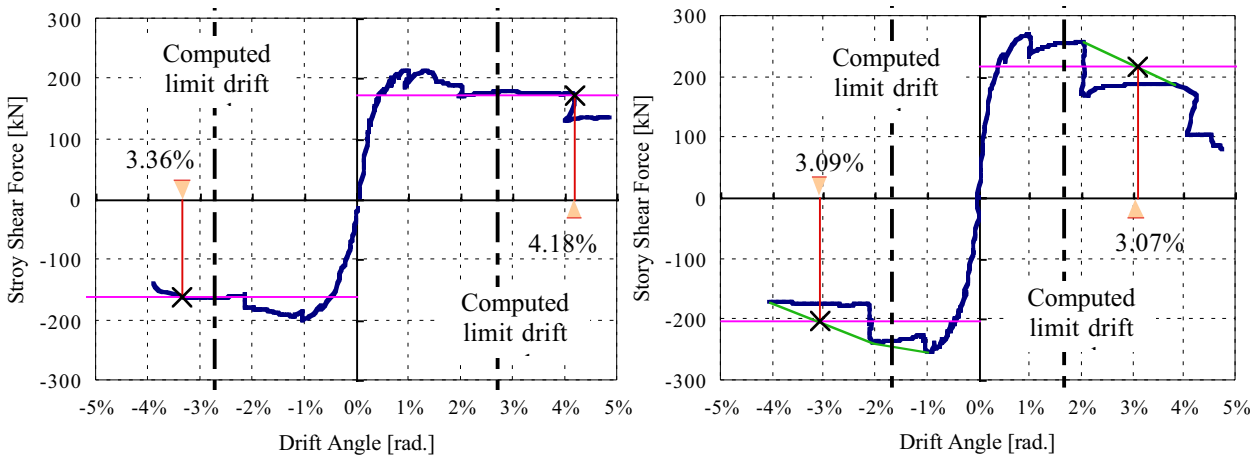

(a) Specimen No.1 (b) Specimen No.2

Fig. 10 Ultimate limit drift angle obtained in test and computation

limit deformations based on the F index for both specimens were conservative comparing with test results. Ultimate limit drift angle for Specimen No.2 can be supposed to be 2 % approximately if the effect of cyclic load reversals on seismic resistant performance is taken into account, because significant lateral resistance degradation occurred after the drift angle of 2 %. Then predicted ultimate limit drift angle of 1.68 % for Specimen No.2 seems to be adequate.

3.5 Energy Dissipation

The equivalent viscous damping ratio for each loading cycle in story shear force - drift angle relations is shown in **Fig. 11**. The equivalent viscous damping ratio was calculated by normalizing the dissipated energy within half a cycle by the strain energy at peak of an equivalent linearly elastic system. The equivalent viscous damping ratio in Specimen No.1 was smaller than 10 % at the drift angle less than or equal to 1 % and increased rapidly to 20 % at sixth loading cycle with the formation of beam hinge mechanism. The equivalent viscous damping ratio in Specimen No.2 exceeded 10 % even at second loading cycle corresponding to the drift angle of 0.5 % since all longitudinal bars yielded in the R/C edge column beside a steel brace. The equivalent viscous damping ratio in Specimen No.2 was greater than that in Specimen No.1 for all loading cycles. Therefore it is pointed out that the entire flexural failure at the bottom of a multi-story steel brace absorbed more hysteresis energy than the uplift rotation failure.

Cumulative energy dissipation is shown in **Fig. 12**. The amount of cumulative energy dissipation for Specimen No.2 was by 113 percent greater than that for Specimen No.1 at the drift angle of 1 % at which the peak lateral strength was achieved, and by 50 percent greater than that for Specimen No.1 at the last loading stage.

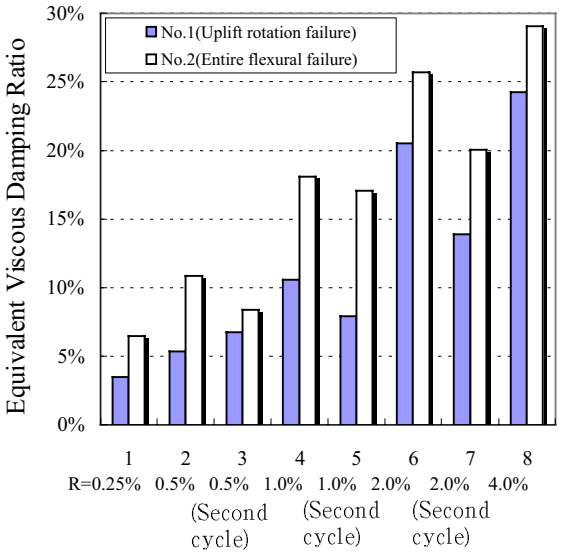

Fig. 11 Equivalent viscous damping ratio

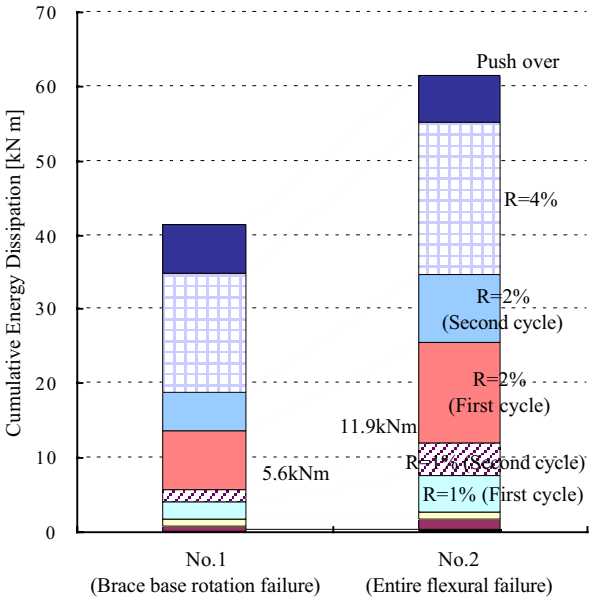

Fig. 12 Cumulative energy dissipation

5. EARTHQUAKE RESPONSE ANALYSIS

Nonlinear static and earthquake response analyses were carried out for a R/C space building strengthened by a multi-story steel brace which was designed to cause the base uplift rotation of the brace. Effect of bi-directional horizontal loads on the earthquake response of the strengthened building, restraining action to the uplift of a multi-story steel brace by transverse beams framing into R/C edge column beside the brace, and induced axial forces in R/C edge column were studied in the analyses. Three-dimensional frame analysis was executed by the computer program called CANNY-E.

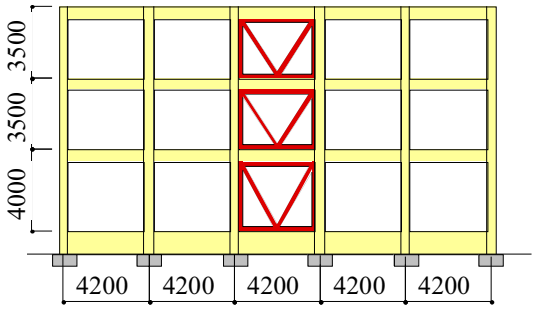

(a) Elevation of Y2 frame

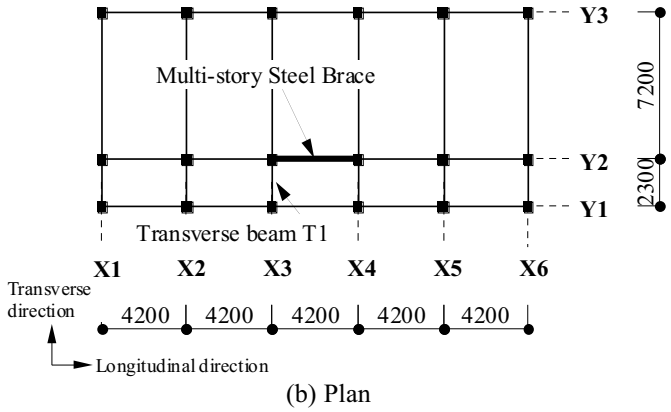

(b) Plan

Fig. 13 R/C Building for analysis

5.1 Building for Analysis

A three-story R/C school building with five bays of each 4200 mm span length in longitudinal direction and two bays in transverse direction shown in **Fig. 13** was used for the analyses, which was designed according to previous seismic provisions in

Table 4 Cross sections of members (Unit in mm)

(a) Beam (R : Plain bar)

Floor level		Ground	Second	Third	Roof
Longitudinal direction	Top	4-R25	5-R22	4-R22	3-R19
	Bottom	4-R25	4-R22	3-R22	2-R19
	Section	300 x 1100	300 x 600		
Transverse direction	Top	4-R25	5-R22	4-R22	4-R22
	Bottom	4-R25	2-R22	2-R22	2-R22
	Section	300 x 1100	300 x 800		

(b) Column (R : Plain bar)

Section dimension	450 x 500
Longitudinal bar	14-R25
Hoop	2-R9@250

(c)Brace

Section	H-200 x 200
Flange thickness	12
Web thickness	8

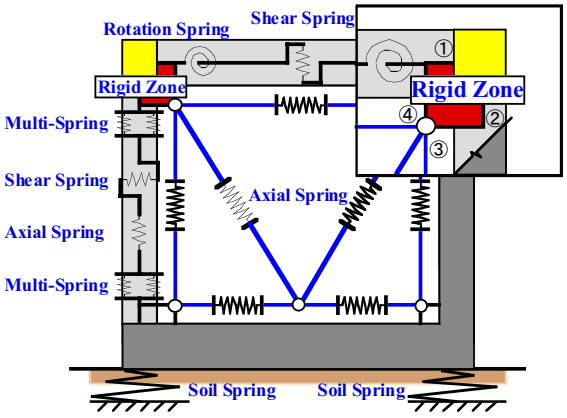

Fig. 14 Modeling for R/C members and steel brace

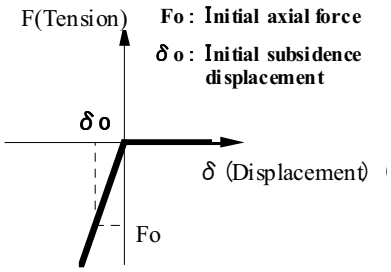

Fig. 15 Envelope curve for soil spring

Japan. Cross sections of R/C beams and columns are shown in **Table 4**. One multi-story steel brace having H-shaped cross-section with 200 mm width and 200 mm depth was placed at the center of the building.

5.2 Modeling of Members

Each R/C member and steel brace is modeled as shown in **Fig. 14**. The inelastic hinge region at the top and the bottom of columns was represented by the multi-spring (MS) model [3]. Beam member was represented by a one-component model, in which an inelastic rotation spring ruled by Takeda hysteresis model was placed at both beam ends and an inelastic shear spring ruled by Origin-oriented hysteresis model at the beam center. Steel yield strength was 235 N/mm^2 and concrete compressive strength was 21 N/mm^2.

The horizontal, vertical and diagonal steel chords of a brace were modeled as the axial spring with pins at both ends. The steel brace was connected to R/C members at four corner points by a pin. Therefore, the entire flexural failure at the bottom of a multi-story steel brace, depending on the pull-out of anchorage bars connecting horizontal steel rim and R/C foundation beam, can not be represented in this model. Soil springs, which do not resist tensile force as shown in **Fig. 15**, were placed under the foundation to cause the uplift of a multi-story steel brace.

5.3 Static Analysis

Story shear force - story drift relations are shown in **Fig. 16** in uni-directional static analysis to longitudinal direction, providing lateral loads of an inverted triangular distribution shape along the height of a building. Solid circle represents the occurrence of uplift of R/C edge column beside the brace. This coincides with the point that the axial force of the soil spring beneath the column reaches zero from compression. Lateral resistant capacity of the strengthened building with transverse beams framing into a multi-story steel brace was enhanced to 1.15 times that without transverse beams by restraining effect of transverse beams on the uplift rotation of a multi-story steel brace.

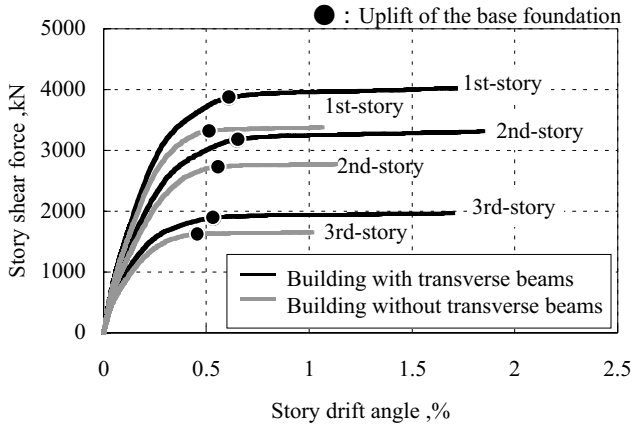

Fig. 16 Story shear force - drift angle relations

5.4 Earthquake Response Analysis

Uni- and bi-lateral earthquake response analyses were carried out using JMA Kobe motion records in Hyogo-ken Nanbu Earthquake (1995) shown in **Fig. 17**. EW component of the records was input to the longitudinal direction of three-dimensional building in uni-lateral analysis. EW and NS components were input to the longitudinal and transverse direction respectively of the building in bi-lateral analysis. Newmark Beta method was used in numerical integration. Viscous damping matrix was assumed to be proportional to instantaneous stiffness matrix, and the initial elastic damping factor for the first mode vibration was chosen to be 5 % of the critical.

First-story shear force - drift relations in longitudinal direction are shown in **Fig. 18**. Solid circle represents the occurrence of uplift of a multi-story steel brace and solid square the flexural

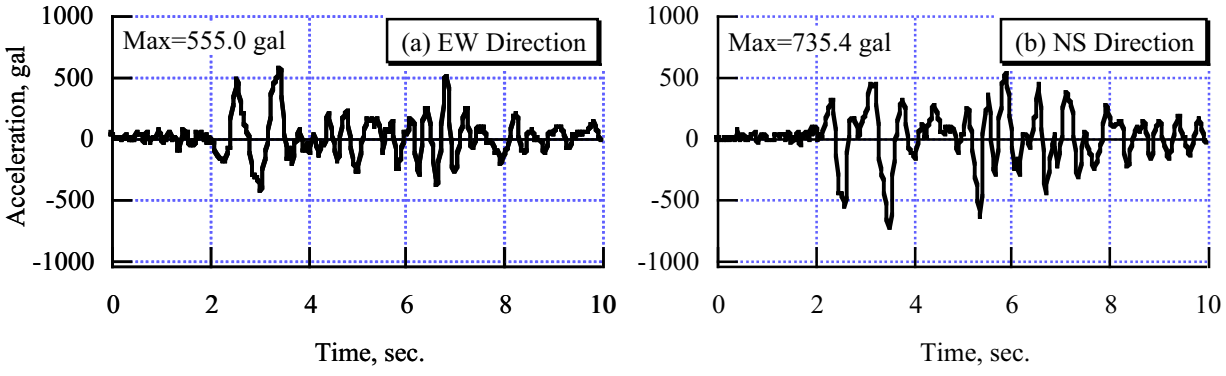

Fig. 17 Hyogo-ken Nanbu Earthquake motion records

yielding of R/C foundation beam framing into the brace in transverse direction. For bi-lateral earthquake response, transverse foundation beam yielded prior to the uplift rotation of a multi-story brace since NS component of earthquake motion excited the response in transverse direction. Thereafter, first-story stiffness was degraded gradually. First-story drift of longitudinal direction in bi-lateral earthquake response increased to 2.4 times that in uni-lateral earthquake response, exceeding the drift angle of 2 %. On the contrary, first-story drift in uni-lateral earthquake response did not exceed the drift angle of 1 % because shear force induced in transverse beams contributed entirely to restrain the uplift rotation of a multi-story steel brace.

Lateral resistance of longitudinal direction was by 10 percent smaller in bi-lateral earthquake response than that in uni-lateral earthquake response. This was caused by the reduction of restraining effect of transverse beams on the uplift of the brace since resisting moment of transverse beams resulting from NS ground motion cancelled occasionally the moment which can contributes to restrain the uplift of the brace.

Interactions between bending moment and axial force induced at the bottom of R/C edge column adjacent to steel brace in first-story, where the uplift of a multi-story steel brace occurred, are shown in **Fig. 19**. Bending moment in bi-lateral earthquake response was by 50 percent greater in longitudinal direction and by 30 percent smaller in transverse direction than that obtained in uni-lateral earthquake response

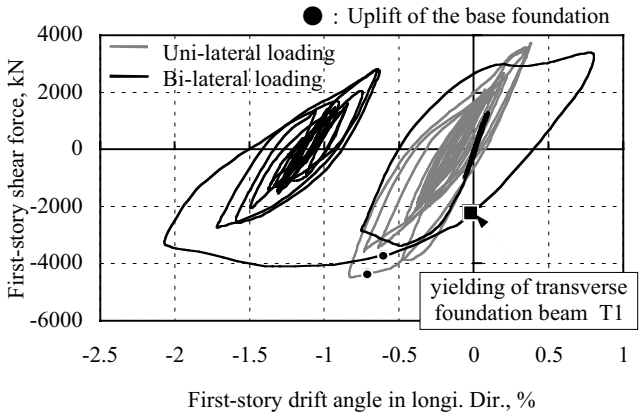

Fig. 18 Earthquake response of first-story shear force and drift in longitudinal direction

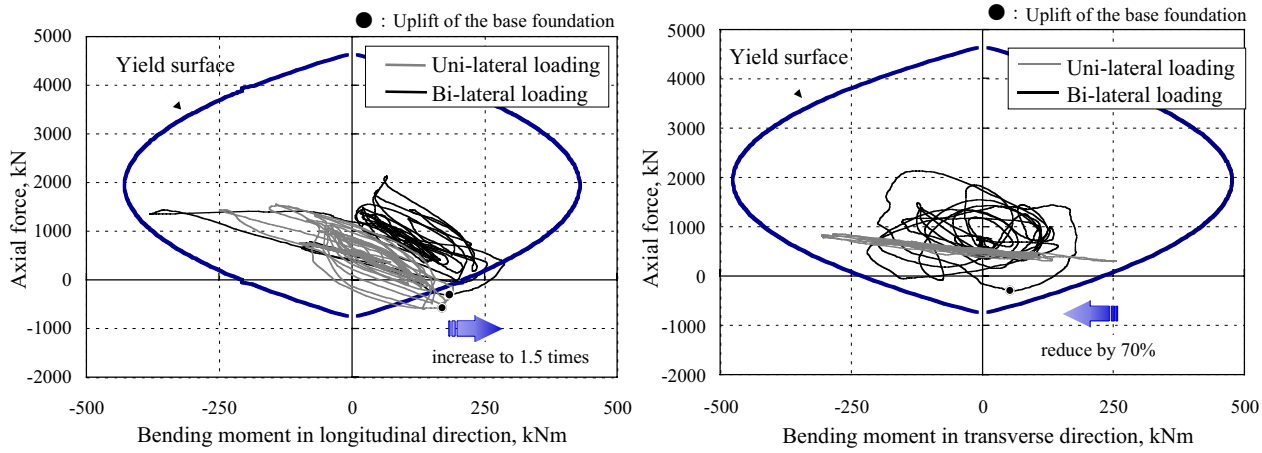

Fig. 19 M-N Interaction of R/C edge column beside brace

analysis. This was attributed to varying column axial force in bi-lateral earthquake response analysis from tension to compression corresponding to the axial stress ratio of 0.45 to concrete compressive strength.

6. CONCLUSIONS

Earthquake resistant performance in plane R/C frames strengthened by a multi-story steel brace was investigated through the tests under cyclic load reversals focusing on the base uplift rotation of the brace and the entire flexural failure at the bottom of the brace caused by tensile yielding of all longitudinal bars in a R/C edge column. Earthquake response was studied by three-dimensional frame analyses of strengthened R/C building subjected to bi-lateral earthquake motions. The following concluding remarks can be drawn from the present study:

(1) Lateral resistance for the base uplift rotation of a multi-story steel brace decreased gradually after flexural yielding occurred at the end of boundary beams and the bottom of first-story isolated columns at the drift angle of 1.4 %. Lateral strength computed by taking account of restraining effect of both boundary and foundation beams on uplift rotation agreed well with the test result.

(2) For the specimen failed in entire flexure at the bottom of a multi-story steel brace, all longitudinal bars in a R/C edge column subjected to tension beside the brace yielded at the drift angle of 0.3 %. Hysteresis loops showed a spindle shape until the drift angle of 2 %, stably dissipating hysteresis energy. However lateral resistance diminished abruptly by concrete crushing and fracture of column longitudinal bars at the bottom of both edge columns. Lateral strength computed by considering both flexural resistance attributed to tensile force in a R/C edge column and resisting moment of boundary beams same as the case of the base uplift rotation underestimated a little that obtained in the test. Contribution of the vertical steel rim to the entire flexural resistance should be taken into account if anchorage of the bottom of a multi-story steel brace to R/C foundation beam is sufficient to carry tensile axial force in vertical steel rim to the foundation.

(3) Ultimate limit deformations in two specimens estimated by considering respective deformation ability of boundary beams and an isolated steel brace were conservative comparing with test results.

(4) Ductility performance in the brace uplift rotation failure was superior to that in the entire flexural failure due to tensile yielding of all longitudinal bars in a R/C edge column.

(5) The amount of energy dissipation in the entire flexural failure at the bottom of a multi-story steel brace was by 50 percent greater than that in the brace uplift rotation failure.

(6) It is judged that earthquake resistant performance of strengthened R/C frames which is controlled by the entire flexural failure at the bottom of a multi-story steel brace is superior to that in the brace uplift rotation failure within the range of the drift angle of 2 %.

(7) Lateral resistant capacity of strengthened building with transverse beams framing into a multi-story steel brace for uni-lateral static frame analysis was enhanced to 1.15 times that without transverse beams by restraining effect due to transverse beams on the uplift rotation of the brace.

(8) First-story drift of longitudinal direction parallel to the brace in bi-lateral earthquake response increased to 2.4 times that in uni-lateral earthquake response, caused by the reduction of restraining moment of transverse beams.

ACKNOWLEDGMENT

The study reported in the paper was sponsored by a Grant-in-aid for Scientific Research of Japan Society for the Promotion of Science (Head researcher : K. Kitayama). The test was executed by Mr. H. Kato, Rui Design Room Co.Ltd, as a part of the master thesis in Tokyo Metropolitan University.

REFERENCES

[1] Kato, D., H. Katsumata and H. Aoyama : Effect of Wall Base Rotation on Behavior of Reinforced Concrete Frame-Wall Buildings, Proceedings of the Eighth World Conference on Earthquake Engineering, San-Francisco, July, 1984.

[2] Japan Building Disaster Prevention Association : Standard for Evaluation of Seismic Capacity of Existing Reinforced Concrete Buildings, revised in 2001, (in Japanese).

[3] Lai, S.S., G.T.Will and S. Otani : Model for Inelastic Biaxial Bending of Concrete Members, Journal of Structural Engineering, ASCE, Vol.110, No.11, pp.2563-2584, November, 1984.